Low-frequency acoustic emission characteristics from meter-scale fracturing of rock-like brittle materials

June-Ho Park
Korea Advanced Institute of Science and Technology, Daejeon, Republic of Korea

Jin-Seop Park
Korea Atomic Energy Research Institute, Yuseong-gu, Daejeon, Republic of Korea

Chang-Ho Hong
Korea Atomic Energy Research Institute, Yuseong-gu, Daejeon, Republic of Korea

Ji-Won Kim
Korea Atomic Energy Research Institute, Yuseong-gu, Daejeon, Republic of Korea

Tae-Hyuk Kwon
Korea Advanced Institute of Science and Technology, Daejeon, Republic of Korea

ABSTRACT: The acoustic emission (AE) method as a passive non-destructive monitoring technique is proposed for real-time monitoring of mechanical degradation in underground structures, such as deep geological disposal of high-level nuclear waste (HLW). This study investigates the low-frequency characteristics of AE signals emitted during fracturing of meter-scale concrete specimens. For comparison, uniaxial compression tests (UCT) and Goodman jack (GJ) tests in a 1.3 m-long concrete block were conducted while acquiring the AE signals using low-frequency AE sensors. The results showed that a sharp increase in AE energy emission occurred at ~60% and ~80% of the yield stresses in the UCT and GJ tests, respectively. High frequency AE signals were captured more as the tress increased in the GJ tests, which was in contrast to the UCT tests. The study presents unique experimental data with low-frequency AE sensors under different loading conditions, which provides insights into the field-scale AE monitoring practices.

Keywords: Acoustic emission, low-frequency sensor, meter-scale, concrete, Goodman jack test.

1 INTRODUCTION

Acoustic emission (AE) technology is a passive-type non-destructive monitoring method which captures and analyzes the emitted elastic waves from material deformation and failure (Grosse & Ohtsu 2008 and Aggelis et al. 2013). This AE method has been widely used to acquire additional but useful information from lab-scale experiments, and recently it has been adopted for large structural monitoring in engineering practices, such as bridges, pipes, and storage tanks. Accordingly, AE is also proposed for monitoring of underground geologic structures, including geologic disposal of high-level nuclear wastes (Falck & Nilsson 2009, Kim et al. 2011 and Choi et al. 2014).

Previous studies have examined the AE characteristics and parameters (AE energy, count, RA value, average frequency, and peak frequency) as well as crack mode classification with various concretes and rocks which are considered as brittle materials (e.g., Federation of Construction Material Industries 2003, Ohtsu et al. 2007, Ohno & Ohtsu 2010, Aggelis et al. 2013 and Nakamura et al. 2016). Majority of the previous studies has used high-frequency AE sensors greater than 100 kHz with centimeter-scale specimens, however, the field-scale application of AE techniques is

expected to require low-frequency AE sensors less than 100 kHz owing to the large attenuation in fields.

Therefore, this study investigates the low-frequency AE characteristics emitted during two types of mechanical loading tests with concrete specimens. The uniaxial compression tests (UCT) with concrete specimens of 10 cm diameter and the Goodman jack (GJ) test with a 1.3 m-long concrete cube were conducted while acquiring AE signals by using low-frequency AE sensors with a central frequency of 60 kHz. We chose the Goodman jack test (or the borehole test) to examine the effect of specimen-scale and loading type as comparison to the UCT testing because it is typically used to investigate *in situ* rock deformability in excavation-induced damage zones in fields (McElroy et al. 1985, Goodman 1989, Palmstrom & Singh 2001 and Singh 2011). Concrete was selected for its brittle nature and ease of creating well-controlled specimens. The analyzed AE parameters include the AE count, AE energy, RA value (the ratio of rise time to max amplitude), average frequency (the ratio of count to duration in the time domain, and the peak frequency in the frequency domain. The study reports unique low-frequency AE data and compares their characteristics with respect to their loading conditions, which advances our understanding for practical applicability and scalability of AE techniques to a larger scale.

2 MATERIALS AND METHODS

This study prepared concrete specimens based on the recipe used in the Korean low-level radioactive waste disposal structures, as shown in Table 1. The specimens for UCT had a cylindrical shape with a diameter of 100 mm and a height of 200 mm, and the AE sensor locations are illustrated in Figure 1. The load was applied at 0.2 mm/min using a hydraulic loading frame with a capacity of 1000 kN. During UCT tests, the lateral and vertical strains were measured using a biaxial strain gauge (Model KFG-10-120-D16-11L1M2S, Kyowa, Japan). From the UCT, the maximum (peak) stress was determined as the yield stress, and the AE analysis was performed with the data up to the peak stress.

The cubic specimen with a side of 1.3 m was prepared, which housed one borehole with a diameter of 80 mm and a depth of 500 mm for the GJ tests, as shown in Figure 2. A hand pump applied force at 4 MPa/min through a hard-rock jack and two LVDTs mounted at bearing plates recorded the displacements in the borehole (Model GJ-75, ACE Inst., Korea). The average of the near and far displacements was used in this study. The GJ test with jacking was carried out two times, horizontal and vertical directions each, at the borehole depth of 100 mm. The jacking was halted when the jacking pressure reached 30 MPa.

During the UCT and GJ tests, we collected AE signals by using eight AE sensor with a resonant frequency band of 60 kHz (Model AE603SW-GA, Rectuson, Korea) with the AE acquisition system (Model μDISP MISTRAS, PAC, U.S.A).

Table 1. Composition of the concrete specimen.

Mix ratio (%wt)									
Water	Cement	Fly ash	Aggregate (<20mm)	Coarse sand (3–5 mm)	Fine sand (0.2–1 mm)	Water reducing agent	Air entraining (AE) agent	Superplasticizer (HR water-reducing agent)	Total
8.01	16.32	4.07	41.6	17.92	12.03	0.0003	0.000036	0.0011	100

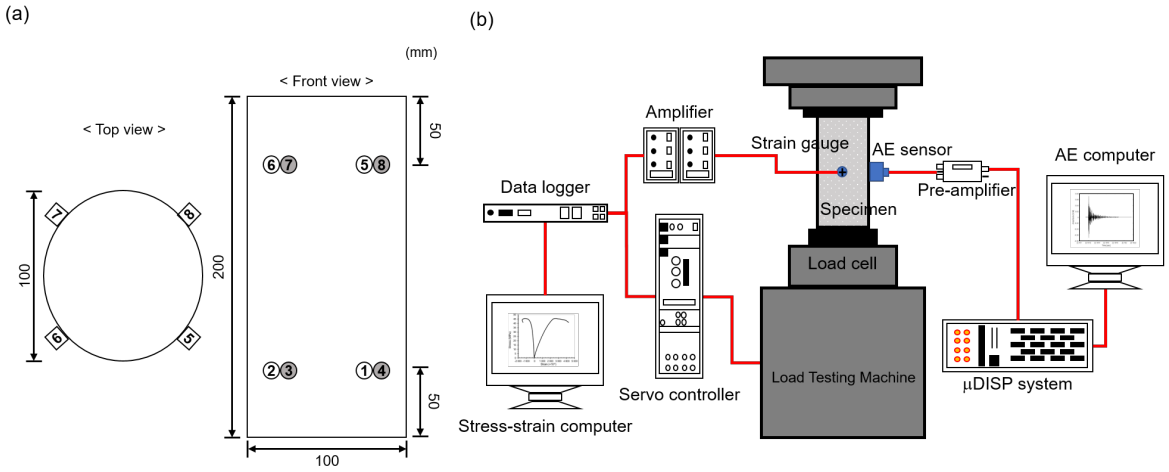

Figure 1. (a) Specimen design of UCT (all dimension is in mm, and numbers in squares or circles indicate the channel of AE sensor.) and (b) a schematic diagram of the measurement system.

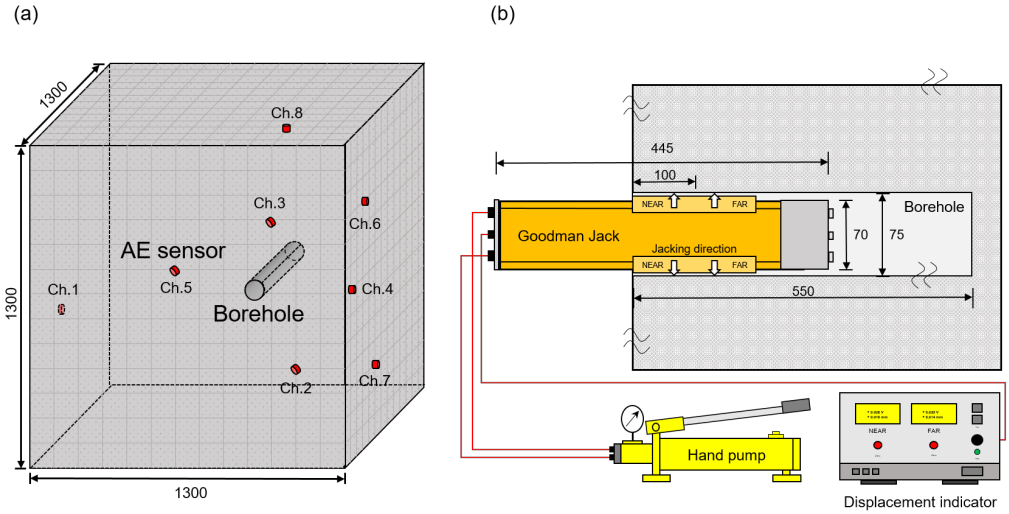

Figure 2. (a) Specimen design of meter-scale test (all dimension is in mm and numbers in squares indicate the channel of AE sensor.) and (b) a schematic diagram of the measurement system.

3 RESULTS

There are two types of AE signal analysis, (1) parameter-based and (2) conventional signal-based methods. In this study, AE count, AE energy, and RA value-average frequency (AF) distribution method are used in the parameter-based method, and peak frequency was used in the signal-based method through Fast Fourier Transform (FFT).

3.1 Time-domain parameters – AE counts and AE energy

In the case of UCT, the strength was yielded at 28 MPa, crack generation and growth actively developed after around 64% of the yield stress, and the collection of AE signals rapidly increased. The total cumulative AE energy was 0.16 V^2·sec, and Figure 3(a) confirmed that 72% of total AE energy was measured at this point. BH_100_hor and BH_100_vert require time to stabilize after a certain amount of pressure due to the characteristics of hand pumps. Therefore, it can be confirmed that a lot of AE signals are collected during the pressurization period. In Figure 3(b), the pressing

direction was horizontal, and the final displacement at the end of the experiment was 0.76 mm. Many AE signals were collected during the last three pressurization processes. It was confirmed that more than 58% of the total cumulative AE energy of 0.33 V^2·sec was collected after 80% of the total displacement. In the Goodman jack experiment conducted after that, the pressing direction was changed from horizontal to vertical, the final displacement was 0.78 mm, and the total cumulative AE energy was 0.31 V^2·sec, which can be confirmed through Figure 3(c). After 81% of the final displacement, over 52% of the total measured AE energy was collected. Hence, it has been observed that the point at which AE energy accumulated rapidly was delayed from approximately 60% to 80% when scaling up from lab to meter scale. The trend of AE event collection differed from the Goodman jack tests, where loads were applied at the same depth in different directions. Nevertheless, the tendency of cumulative AE energy was consistent, thus confirming the reliability of AE factor analysis. This finding highlights the importance of considering scale effects when analyzing AE data from laboratory-scale tests for practical field applications.

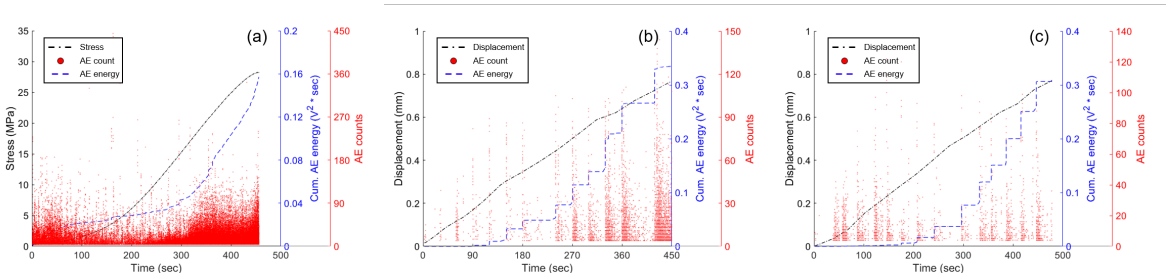

Figure 3. The variation in stress or displacement, cumulative AE energy, and AE counts over time of test cases: (a) uniaxial compression test (UCT), (b) borehole test in the horizontal direction (BH_100_hor), and (c) vertical direction (BH_100_vert).

3.2 Frequency-domain parameters – Peak frequency

Figure 4 shows the normalized density for the peak frequency. The peak frequency was mainly in the range of 4–28 kHz and 56–80 kHz. In the case of UCT, more than 97% of the collected AE signals were distributed in the low-frequency band, as shown in Figure 4(a). Figure 4(c) shows that more than 88% of the BH_100_vert was distributed in the low peak frequency group. As shown in Figure 4(b), 46% of the signals were distributed in the high-frequency group only for BH_100_hor, and about 50% were distributed in the low-frequency group. Repeating the experiment at the meter scale revealed a difference in the peak frequency distribution, particularly in the high-frequency band when the experiment was conducted at the exact load location. This observation suggests a gradual convergence toward the lab-scale results. Consequently, a different criterion for analyzing the peak frequency on low-frequency AE sensors would be necessary to detect the initial structural deterioration in situ field settings.

Figure 5(a)–(c) shows the peak frequency distribution according to the degradation stage. In Figure 5(a), most of the signals corresponding to the high-frequency group were collected in the range of 10 MPa or less, and signals corresponding to the low-frequency group were collected in large quantities from the beginning of the test to the point of failure. In contrast, in BH_100_hor, most of the signals included in the high-frequency group were collected after 17 MPa, and the low-frequency group was collected from the beginning. In the BH_100_vert performed after that, signals corresponding to the high-frequency group were hardly caught again, and about 4% of the total collected signals were collected after 20 MPa.

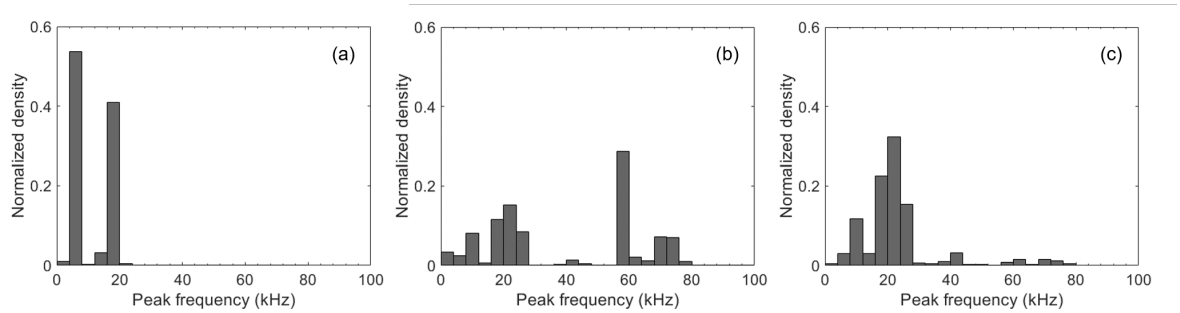

Figure 4. The variation in peak frequency is expressed as normalized density: (a) uniaxial compression test (UCT), (b) borehole test in the horizontal direction (BH_100_hor), and (c) vertical direction (BH_100_vert).

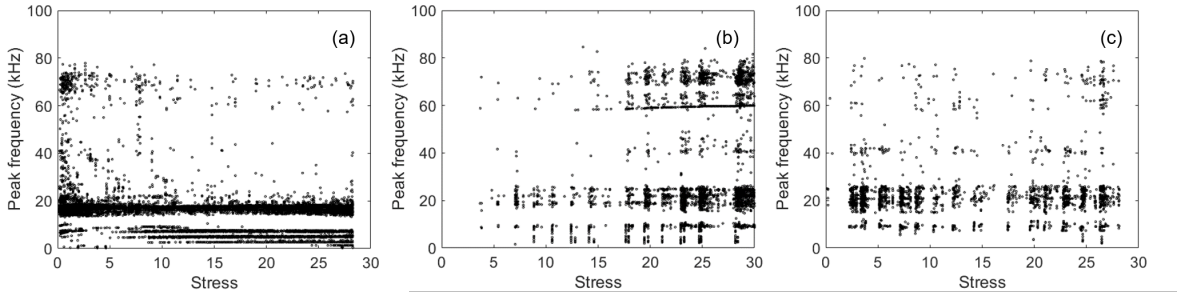

Figure 5. The variation in peak frequency over stress: (a) uniaxial compression test (UCT), (b) borehole test in the horizontal direction (BH_100_hor), and (c) vertical direction (BH_100_vert).

3.3 RA value and Average frequency

Figure 6 shows the variation in average frequency and RA value. In the UCT case, the average frequency was mainly distributed between 0–100 kHz, and the RA value was distributed between 0–3.5×10^5 μs/V. Even in the BH_100_hor case, the average frequency was distributed in 0–100 kHz, and the RA-value was mostly distributed in 0–2.0×10^5 μs/V. Most of the AE signals of BH_100_vert had an average frequency of 0–60 kHz and an RA-value of less than 5.0×10^5 μs/V. The AE signals obtained from the Goodman jack tests tended towards smaller RA values compared to those obtained from the UCT results. Additionally, the maximum value of the average frequency also exhibited a decreasing trend.

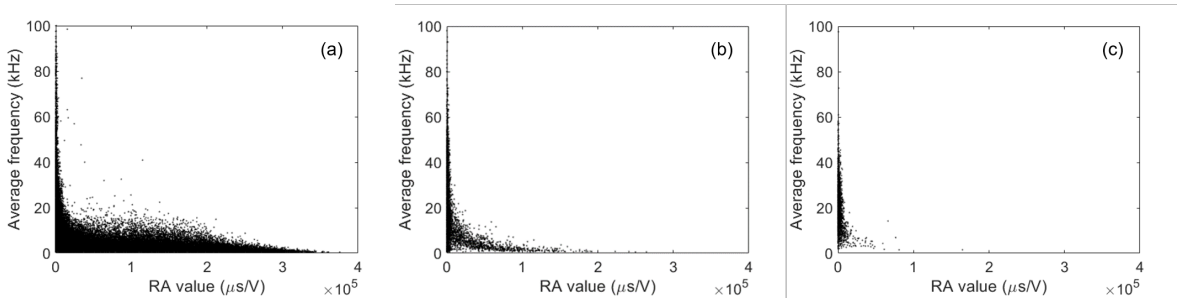

Figure 6. The variation in average frequency over RA value: (a) uniaxial compression test (UCT), (b) borehole test in the horizontal direction (BH_100_hor), and (c) vertical direction (BH_100_vert).

4 CONCLUSION

This study investigated the characteristics of AE factors during failure using a low-frequency AE sensor. A uniaxial compression test (UCT) and borehole tests (Goodman jack tests) were conducted.

AE analysis was performed on factors such as AE count, peak frequency, average frequency, RA value, and AE energy. The results showed that the cumulative AE energy grew significantly before the yield stress was reached. This result verifies the dependability of the AE factor analysis, emphasizing the significance of accounting for scale effects when evaluating AE data for in situ applications based on laboratory-scale tests. The collected AE signals were primarily contained in two frequency bands: in the range of 4–28 kHz and 56–80 kHz. Through comparing peak frequency analysis results, we confirmed that establishing an alternative criterion for analyzing the peak frequency on low-frequency AE sensors is critical to effectively detect the initial signs of structural deterioration in field settings. The AE signals collected from the Goodman jack tests demonstrated a tendency towards lower RA values than the UCT results. Furthermore, the maximum average frequency demonstrated a decreasing trend, reaching a maximum value. The RA value was found to be a possible standard for plastic deformation.

ACKNOWLEDGMENTS

This research was supported by Underground City of the Future program funded by the Ministry of Science and the National Research Foundation of Korea (NRF) grant funded by the Korea government (MSIT) (NRF-2022M3E9A1099450).

REFERENCES

Aggelis, D. G., Mpalaskas, A. C., & Matikas, T. E. (2013). Investigation of different fracture modes in cement-based materials by acoustic emission. *Cement and Concrete Research, 48*, 1-8.

Choi, H. J., Kim, K. S., CHo, W. J., Lee, J. O., and Choi, J. W. (2014), *"HLW Long-term Management System Development: Development of Engineered Barrier System Performance", Korea Atomic Energy Research Institute Report,* KAERI/TR-3859.

Falck, W. E., and K. F. Nilsson. "Geological disposal of radioactive waste: moving towards implementation." *JRC reference report* (2009).

Federation of Construction Material Industries. (2003). *Monitoring Method for Active Cracks in Concrete by Acoustic Emission, JCMS-III B5706,* 23-28.

Grosse, C. U., & Ohtsu, M. (Eds.). (2008). *Acoustic emission testing.* Springer Science & Business Media.

Kim, J. S., Kwon, S. K., Sanchez, M., & Cho, G. C. (2011). Geological storage of high level nuclear waste. *KSCE Journal of Civil Engineering,* 15(4), 721-737.

Nakamura, H., Ohtsu, M., Enoki, M., Mizutani, Y., Shigeishi, M., Inaba, H., ... & Sugimoto, S. (2016). *Practical acoustic emission testing* (pp. 66-69). Tokyo, Japan: Springer.

Ohno, K., & Ohtsu, M. (2010). Crack classification in concrete based on acoustic emission. *Construction and Building Materials*, 24(12), 2339-2346.

Ohtsu, M., Isoda, T., & Tomoda, Y. (2007). Acoustic emission techniques standardized for concrete structures. *Journal of Acoustic Emission, 25*(2007), 21-32.

Ouyang, C., Landis, E., & Shah, S. P. (1991). Damage assessment in concrete using quantitative acoustic emission. *Journal of Engineering Mechanics, 117*(11), 2681-2698.

Wang, Y. S., Deng, J. H., Li, L. R., & Zhang, Z. H. (2019). Micro-failure analysis of direct and flat loading Brazilian tensile tests. *Rock Mechanics and Rock Engineering, 52*, 4175-4187.

Zhang, Z. H., Deng, J. H., Zhu, J. B., & Li, L. R. (2018). An experimental investigation of the failure mechanisms of jointed and intact marble under compression based on quantitative analysis of acoustic emission waveforms. *Rock Mechanics and Rock Engineering, 51*, 2299-2307.